Chapter 3

Experimental

3.1 Introduction

The experimental methodologies adopted in the present work to study the Ti6Al4V-SiC$_f$ composite are resulted useful in a point of view both microscopic and macroscopic, about both typologies of composite analyzed.

The microchemical and microstructrural examinations have allowed to determinate the real evolution of the diffusion atomic elements and to analyse possible anelastic phenomena, especially on the fiber-matrix interface. This experimental study has been developed by high precision instrumentation, so as to have accurate results to compare with theories.

By the mechanical probes it has been possible to characterize the composite behaviour under stress, both during high application temperature and at high vibrational capacity.

Especially the first part of the used experimental techniques is explained in this section as first introduction, to make clear their concepts to a better result understanding. To that the description follows about the typologies of carried tests and of the adopted instrumentation to the present studies.

3.2 Micro-chemical spectroscopic techniques

The scientific literature demonstrates the existence of a large number of experimental techniques that allow the study of a sample through the properties that characterize it.

The major part of this techniques bases their applications on the interpreting the reaction that the specific sample gives when stimulated with an appropriate energy. The energy levels and the reaction type determine the investigation typology that is performed.

The spectroscopic techniques, used during the course of this argument, utilize the electron emission processes caused by an electrons source (AES and SEM) or a photons

source (XPS) by appropriate energy. The differences between these spectroscopic techniques reside in different processes of quantum nature that involve the system studied. As a result these techniques carry out investigation on different portions of the specific studied surface (Fig.1).
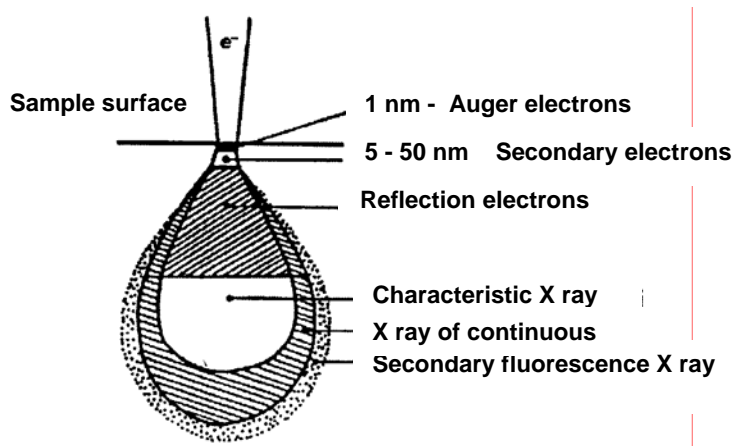

Fig.1 Pattern of particles involved in emission in the sample volume

3.2.1 Electron microscopy

The scanning electron microscopy (SEM) is a technique widely used investigation to determine the surface morphology of a sample. When a beam of high energy electrons affect the surface of a sample, starts a series of mechanisms that cause the release of several types of signals due to reflection electrons, secondary and Auger electrons, fluorescence X and other photons with different energies (Fig.1). The interactions can be divided into two categories:

A) elastic collisions: the primary electron beam changes its trajectory, but it keeps his energy. The impacts are quite violent, as to have a change in the trajectory of 180 ° respect to the primary beam. The probability of an electron to be reflected primary is proportional to the charge of the material. Therefore the amount of signal to reflection electrons depends on the atomic number of analyzed material. The information that we provide the reflection electrons is associated to the distribution of chemical elements in the sample;

B) anelastic collisions: the primary electron beam loses energy by transferring it to the material. One of the phenomena associated to anelastic collisions is the creation of secondary electrons generated by interaction between the primary electron beam and conduction electrons weakly bound in the solid. Measuring the intensity of secondary electrons as a function of the position of the primary beam through the SEM microscope, an sample surface image can be reconstructed by exploiting the fact that the secondary

electron intensity depends on the topography of the sample surface. In addition to the creation of secondary electrons, the primary electron beam interacts with the atom electrons exciting to levels with higher energies. The dis-excitation of electrons cause the emission of X-ray. X-rays can be emitted by generating a continuous background of X-rays (Brehmstrahlung) and a leap in the atomic level atoms that gives the spectrum of characteristic X-rays, typical of sample elements. The wavelength of the characteristic X-rays have power equal to the difference between the initial and final state.

3.2.2 X-ray Photoelectron Spectroscopy (XPS)

The XPS spectroscopy uses the photoelectric effect to obtain information. Known as the photoelectric effect arises by the interaction radiation-material, about that electrons can be extracted from a material through a photons source. The mechanism on that the photoemission process bases is: a photon is absorbed by the atom A, which in turn expels an electron in a vacuum. By an appropriate collection and dispersal system the kinetic energy of electronics photoemission is measured. The process, therefore, can be shown as:

$$A + h\nu \rightarrow A^+ + e^- \qquad (1)$$
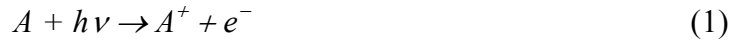
The conservation law of total energy requires that:

$$E(A) + h\nu = E(A^+) + E_k(e^-) \qquad (2)$$

By arrangement:

$$E_k(e^-) = h\nu + [E(A^+) - E(A)]. \qquad (3)$$

The difference in energy between the final ionized state and that initial neutral is called Binding Energy (BE) of electronics photoemission. The equation (3) is not complete because you must introduce the factor ϕ (work function) that considers the necessary work to bring the electron in a vacuum.

$$E_k = h\nu - E_b - \phi \qquad (4)$$

E_k is the energy of the is the photoemission kinetic energy, $h\nu$ exciting radiation and E_b is the electron binding energy in the solid.

The equation (4) is valid in the photoemission process of elastic type. Therefore within the X-rays field will present a series of peaks that reflect the electron binding energy in solid. The binding energy depends on the ion chemical nature, on the type of atomic orbital in that the gap has created. If you want to compare the experimental values of

electronic BE levels of an atom with the orbital energy theory, it should be noted that the first refer to the Fermi level of the solid and the second to the vacuum level.

The photoemission process is anelastic if the photo-electron have a change of its energy (usually a loss) between the photoemission and collecting in the spectrometer. The loss of energy can occur through a series of mechanisms that will be discussed later. The effect of radiation photoemission due to the Bremsstrahlung radiation is dominant at low BE, while the effect related to the secondary electrons, resulting by anelastic photoemission, is dominant in low kinetic energy.

The spectroscopic range of each element is characterized by the presence of a number of photoemission peaks, in relation to the number of core present electrons (inner electrons). H and He does not possess Core electrons, can not be identified by XPS spectroscopy.
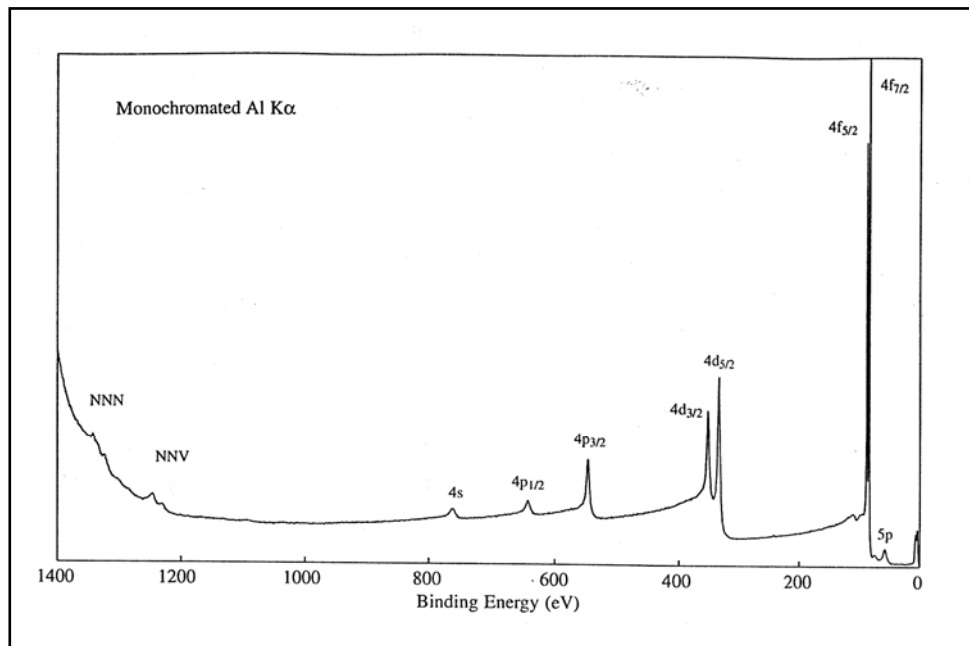

Fig.2 Full scan spectrum of Au excited with a source of Al Kα

Fig.2 is given the full Au spectrum. That spectrum is characterized by a background in which there are peaks, each of which is identified by the specific atomic orbital in according to the bonding energy. In addition to the peaks due to the photoemission process, there are also spikes caused by the process called Auger (NNV, NNN in Fig.2), which mechanism will be discussed in the next paragraph.

Qualitative analysis

Carrying a spectrum in a large BE range, you can identify all the components of the investigated surface. In most cases, the peaks are well resolved and a certain identification allowed, if the element is present in concentrations greater than 0.1 % atomic.

Photoemission spectroscopy offers the possibility to obtain information on the status of a chemical element through the binding energy variation, better known as "chemical shift".

About that the theoretic concepts is not easy to describe, but fortunately the determination of the chemical shift is much easier. This deals to determine the BE value of a signal of an element and to compare it with the BE value of the same elements in a different context. But comparing BE is not as immediate as it seems. The photoemission physical process, as already mentioned, is a ionization process. The extract electron generates in the initial neutral system a positive charge, with the consequent loading of the sample. Of course, wanting to measure BE system neutral, loading must be limited and, if possible, avoided. For this reason, during data acquisition, on the sample a electron flow must be guaranteed that neutralizes the charge. By this way however the definition of zero in the scale of binding energies, is univocal only for conductive samples, as their electrical coupling permits to determine as the zero value for that is experimentally obtained the "Fermi edge", i.e. the Fermi level position, by a carefully cleaned in place by a metal such as Ag. When you verify at non-conductive samples, the problem of zero-setting is not resolved by univocal way, despite the continued refinement of the technique. In fact, the photoemission from insulating samples generates a positive loading on the surface with a consequent shift of all the signals towards higher BE values. The magnitude of that shift is unforeseeable, as it depends not only on the sample nature, but also by the sampling and by the surface of the material. This obstacle can be overcome through the use of a reference signal to a fixed location and well known. Normally it takes as a reference the signal of C 1s rising by the carbon contamination (285.0 eV). In some cases, a flow of low-energy electrons is used to neutralize the charge that forms during the photoemission.

The spectrum acquisition by XPS is complicated by the presence of signals arising from the processes of secondary nature, which sometimes can disturb the interpretation of a XPS signal. But the presence of secondary structures has the advantage of obtaining additional information on the nature of the sample investigated.

Quantitative analysis

The quantitative determination of the various chemical species, expressed as percentages of nuclear and/or atomic relations, is derived from the relationship between the main areas of the reviewed peaks. This intensity ratio must be basically correct for the impact section of photoemission, characteristic for all levels of the individual elements. The methods used for quantitative analysis are two:

-   Method of the sensitivity factors

-   Method of fundamental principles.

The first method is still widely used. It consists to compare the relative intensity of the elements under consideration with those of the peak F1s and C1s (taken as unit), measured directly or indirectly in known stoichiometry compounds. Through these values the measured intensity are correct for the compound under consideration.

The second method allows to get plenty of different atomic species by inductive way. It must take into account several factors: the average free electron path, all compensation due to the trajectories of elastic diffusion, instrumental factors, etc.. The general formula describing the relationship between the current of photoelectrons from a level of an element and the presence of this element in the sample is analyzed as follows:

$$I(E_k,X)=\sigma_i(h\nu,\gamma,X)S(E_k,E_a)\varphi(h\nu)\int_{x=-x_f}^{x_f}\int_{y=-y_f}^{y}\int_{z=0}^{\infty}N_i(x,y,z)\exp\left[-\frac{z}{\lambda(E_k)\cos\vartheta}\right]dxdyd \qquad (5)$$

where:

- $I(E_k,X)$ is the peak intensity on the level of the considered orbital X:

- E_k is the kinetic energy of photoelectrons;

- φ is the flow of ionizing photons;

- σ_i the differential photo-ionization cross section;

- λ is the anelastic average free path of photoelectrons;

- S is the instrumental factor, takes into account both the geometry and the acquisition mode. In this variable is included transmission analyzer and its resolving power, and its sampled area. This feature is specific to each instrument and operating conditions, and it must be determined experimentally;

- N_i is the distribution of the element i into the sample.

Every specific terms are obtained during the specific situation, and their choosing method are beyond by out aim in this work. Only about λ (free medium path) it is possible to say that the value depends mainly by electron kinetic energy and marginally by the chemical and structural nature of the material.

The trend of λ reported as function of photo-electron kinetic energy provides a "universal" curve (Fig.3). If the probability function of electron escape is integrated from zero to 3λ, you get that 95% of the signal comes from this depth.
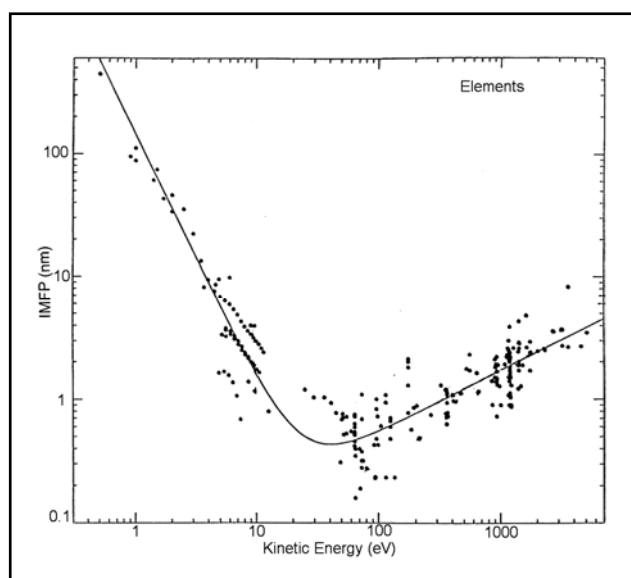

Fig.3 IMFP trend vs. KE

The difference between the two methods is that there may be factors of sensitivity for each geometry, operating conditions and instrument class, which is not possible for the first method that is for one specific situation. Over the estimation of these parameters is more accurate and the result is reliable.

Depth profile

As discussed above, the photoemission spectroscopy XPS obtains information about the chemical and physical nature of the first 1-10 nm of the sample surface. The experimentation may be extended to greater depths by different experimental approaches:

Non destructive process:

A) Fig.3 shows the correlation between the photo-electron kinetic energy and the depth that comes out. It is possible to study the photoelectrons with a greater kinetic energy;

B) If the report to the intensity is expressed as:

$$I_d = I_\infty \, [1 - exp \, (- \, d/\lambda sen\theta)] \hspace{2cm} (6)$$

Where I_d and I_∞ is the intensity of the peak for the thickness d and for infinite. The report concludes that changing the angle of photoelectron collection, you can scan different depths of the samples.

Destructive process:

C) the sample is bombarded by ions of noble gases (with an less energy than 10 keV) which erodes the material, giving the opportunity to study the structure below. Alternating cycles of ion sputtering (this is called the ionic erosion process) by XPS scansion, it is possible to build the depth profile. This procedure involves a careful analysis of the effects that may affect the investigation:

1) preferential sputtering: atoms can be removed with a different rate of erosion, the procedure would produce a variation of artificial stoichiometry of the sample;

2) reduction in the oxidation number of an induced on bombardment, for example $Cu^{2+} \rightarrow Cu^{+}$ or $Sn^{4+} \rightarrow Sn^{0}$;

3) not uniform erosion due to the shade effects for the sample roughness or the presence of surface contamination; uneven distribution of ion beam; bad geometry between the ion beam and the X-ray beam.

By ionic sputtering gives a concentration profile versus erosion time of the sample. The conversion in the scale of depth of the sample analyzed is not immediate because the ion sputtering process is a function of different factors such as incident ion energy Ar^{+}, the eroded surface of the sample, the distance between the sample and ion cannon, etc.., but mainly depends on the type of analyzed material. It is possible to remedy this problem by carrying the profiles on samples of known thickness to obtain the sputtering rate (thickness of eroded sample per minute) at different energies of ions accidents trying to keep the other parameters constant as possible.

3.2.3 Auger Electron Spectroscopy (AES)

Auger spectroscopy is a two-stage process. The first involves the formation of an electronically excited ion, A^{+*}, following the exposure of the sample to a X-rays or electron beam. With a b electron beam the excitation reaction can be written as:

$$A + e^- \rightarrow A^{+*} + e^- + e^-_A \qquad\qquad (7)$$

where e^- is the incident electron from the source, and e^-_A is an electron that has been issued by an internal orbital of A. An atom with an internal electronic gap is unstable, then the process to eliminate this gap begins: an electron from a higher level to the lower level will fall filling the gap, but still leaving the system with a vacancy. At this point this triggers a relaxation process that can take place by two mechanisms in competition with each other:

A) the ion loses another electron from a higher level:

$$A^{+*} \rightarrow A^{2+} + e^{-'}_A \qquad\qquad (8)$$

$e^{-'}_A$ is the kinetic energy of Auger electron. It is given by (9), when the atomic levels involved in the process the level K, which was issued the first electron, the level L_1, from which comes the electron to fill the gap created and the level $L_{2,3}$, from which the second electron:

$$E_{KL1L2,3} = E_K - E_{L1} - E^*_{L2,3} \qquad\qquad (9)$$

$E_{*L2,3}$ is the binding energy level of $L_{2,3}$ in the presence of a potential hole in the internal level L_1.
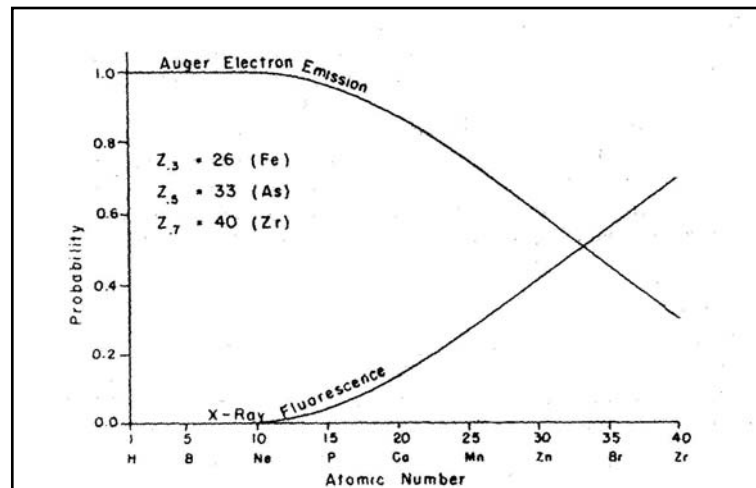

Fig.4 Probability of relaxation through the release of an Auger electron or through the emission of a photon of X-ray energy feature

B) the fluorescence X: the photon emission whose energy is equal to E_K - E_{L1}.

The occurrence probability of one or other process is described by Fig.4

Auger spectroscopy is characterized by its high sensitivity for light atoms, its minimal matrix effects and a high spatial resolution (0.2 μm) which allows you to perform detailed examinations of solid surfaces.

3.4 Internal friction concepts

In a second part of the experimentation internal friction testing have been carried out, whose purpose is to check the mechanical and thermal characteristics of the material, especially in terms of elastic and anelastic behaviour. In particular, the trends of internal friction and elastic modulus as a function of temperature and resonance frequency of the sample have been looked for. It is possible to analyse, in these developments, the presence of a relaxation peak that can indicate any signs of characteristic anelastic phenomena of the material and at what temperature these occur. All this has been developed for the principles that follow.

In fact it possible to say in general that a stress-deformation curve effort about a real material, where there is an application of external load not infinitely slow (as in reality precisely), there is never an immediate adjustment of the system to the variation of this load, but it comfors after a certain period of time. About this condition the following relation stress-deformation values:

$$a_1\sigma + a_2\dot{\sigma} = b_1\varepsilon + b_2\dot{\varepsilon} \tag{10}$$

This relation, due to physical reasons of different nature, implies a clear deviation from the "ideal" elastic behaviour characterized by the Hooke law. This process t of loading and unloading of stress, applied in the range of reversibility, involves dissipation of a quantity of energy, precisely defined internal friction. The result so interesting to go to check for material analysis in the presence of such phenomena dissipative to better simulate the thermo-mechanical real.

It result important to note the correlation between the elastic modulus E with the frequency, that results very useful to determinate the dynamic trend of the studied material during high vibrational work condition. In particular the Young's modulus E is proportional to f^2:

$$f = \frac{m^2 h}{2\pi\sqrt{12}L^2}\sqrt{\frac{E}{\rho}} \tag{11}$$

where m is a constant (m=1.875), L the length of vibrating reed, h its thickness and ρ the material density.

3.5 Microchemical tests

To study by a significant way the concentration of the elements and their diffusion throw the fiber-matrix interface, not only samples at the "as fabricated" state have been analyzing (i.e. at the post- fabrication process condition), but also samples subjected to specific heat treatments in terms of temperature and hours of treatment.

	Temperature (°C)	Exposure time (h)
Pr 1	as fabricated	-
Pr 2	400	100
Pr 3	400	500
Pr 4	400	1000
Pr 5	600	100
Pr 6	600	500
Pr 7	600	1000

Tab.1 Heat treatments of the examined samples

These treatments, indicated in Tab.1, correspond to the working temperatures and times for that applications in components for which the material is candidate.

In addition to the parallel an the perpendicular observation sections, in order to extend the observation zones, surfaces forming a small angle ($\approx 2°$) with the major fiber axis have been prepared by mechanical polishing (Fig.5).

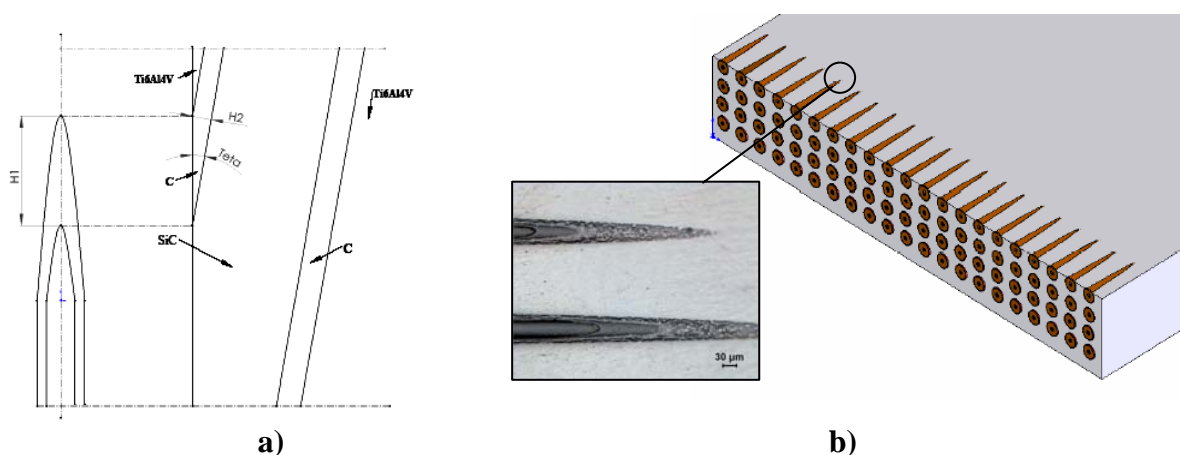**a)**   **b)**

Fig.5 a) Frontal and lateral view of the observed zone b) Sketch of sample preparation.

The results of microstructural investigations have been carried out by means of HT-XRD (X-ray diffraction at high temperature), EDS (Energy Dispersion Spectroscopy), XPS (X-ray Photoelectron Spectroscopy), AES (Auger Electron Spectroscopy). In addition TEM (Transmission Electron Microscopy) observations have been developed.

X-ray diffraction (XRD) measurements have been carried out by using Co-Kα radiation (λ = 0.1789 nm). Precision peak profiles of the most intense XRD reflections have been recorded with angular 2Θ steps of 0.005° and counting time of 20 s per step. The half-height line widths β have been determined and corrected from instrumental broadening. About the most intense reflections of α phase, from the positions of the peaks {100}, {002}, {101}, {102}, {110} and {103} at different temperatures the cell parameters a and c have been determined. For comparison the same tests have been carried out on the monolithic Ti6Al4V alloy.

SEM and EDS experiments were carried out using a Jeol JSM 35 CF microscope.

Photoemission spectra (XPS) have been collected by using a spectrometer ESCALAB MkII (VG Scientific Ltd), equipped with standard Al K$_\alpha$ excitation source and a 5-channeltron detection system. The experiments have been performed at a base pressure of about 1×10^{-10} mbar, that has been increased up to 1×10^{-7} mbar during the depth profiling. The energy of Ar$^+$ ion gun has been set to 3.0 keV and the sample current density – to 2 µA/cm^2. The binding energy (BE) scale was calibrated by fixing the C 1s peak of the graphite at BE = 284.6 eV. The accuracy of the measured BE was $\pm$ 0.1 eV. XPS data were processed by the CasaXPS v.2.2.84 software, using a peak-fitting routine with symmetrical Gaussian–Lorentzian functions. The background was subtracted from the photoelectron spectra by using Shirley method.
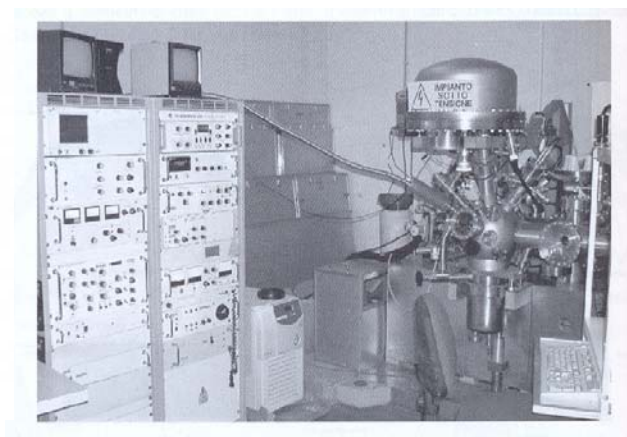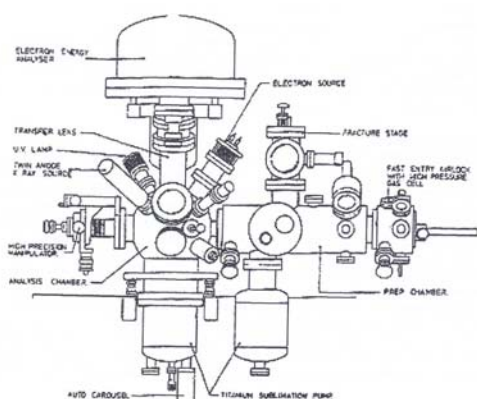

Fig.6 Typical scheme of a device for XPS/AES observation and the ESCALAB MkII spectometer

_____

AES experiments have been performed by using the same spectrometer. The submicron-spot electron gun, a LEG 200, was operated at 10 keV and 1 - 10 nA current. Auger spectra have been registered in a constant retard ratio (1:2) mode, while XPS spectra have been collected at constant analyser energy of 50 eV. A system of slits and electrostatic lens was employed for the measurements in selected-area mode.

Finally, photoelectron chemical images have been obtained by means of a spectrometer Axis Ultra (Kratos Ltd). The principles of the XPS and AES techniques have been described elsewhere [13-15].

To better understand the carbon-titanium interdiffusion occurring at fiber-matrix interface some physical simulations have been carried out. Ti6Al4V (TIMET) and Ti 99.99+ (Alfa Aesar) foils have been coated by thin graphite films (thickness of about 30 nm), heated in vacuum at 500°C for 8 hours and then examined by XPS profiling (Fig.7).

Fig.7 Sketch of the prepared sample to a better physical simulation for diffusion phenomena with the z direction for the XPS profile observation

About the TEM observations the material has been reduced to a thick circular samples having a thickness of 150 μm and diameter of 3 mm. The suitable electrochemical attack, found not without difficulties cause the completely different nature of the two component of the composite, has been constituted by 90 % of methyl alcohol in addition to 10% of perchloric acid, applied by a tension of 10V for 1A of current.

3.6 Mechanical and microstructural tests

The mechanical characterization of composite in as-fabricated condition and after heat treatments has been performed by means of FIMEC (Flat-top Cylinder Indenter for Mechanical Characterisation), tensile and fatigue tests, dynamic modulus and internal friction.

FIMEC is an instrumented indentation test employing a cylindrical punch (Fig.8). Usually the punch has diameter = 1 mm and axial length = 1.5 mm, however, punches of reduced size (diameters up to 0.5 mm) can be used depending on the extension of the zone

to examine. During the test applied load and indentation depth are recorded. Load is divided by contact area so pressure-penetration curves are obtained.

The characteristics of the method have been described in detail in several papers, e.g. [16-19]. When indentation test is carried out with a penetration rate of 1.7×10^{-3} mm s^{-1} or lower, it is possible to compare directly indentation data with those of tensile tests made with a strain rate of 10^{-3} s^{-1}; in these conditions the yield stress $\sigma_y \cong p_Y/3$.
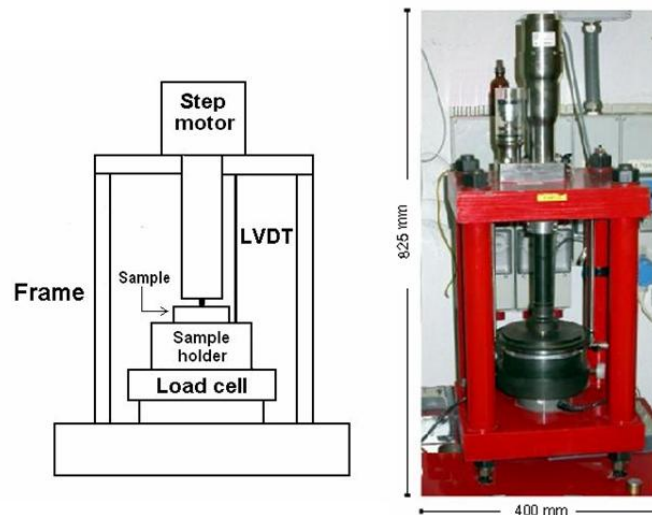

Fig.8 FIMEC instrumentation

The relationship has been verified for a lot of pure metals, alloys and composite materials; the relative difference, $\Delta = (\sigma_Y - p_Y/3) / \sigma_Y$, between $p_Y/3$ values coming from indentation curves and σ_Y values from tensile tests does not exceed 7% , i.e. it is similar to data scattering observed in different tensile tests on the same material [20].

FIMEC tests have been carried on composite and , for comparison, on the monolithic Ti6Al4V alloy at increasing temperature up to 500 °C.

Tensile and fatigue flat-probes (ASTM E21 standard) have been cut from composite sheets. The same probe geometry has been adopted for tensile and fatigue tests (Fig.9). A first group of probes has been tested in the as-fabricated condition while a second group has been heated in vacuum (P = 5×10^{-6} mBar) at 400 and 600 °C for 100, 500 e 1000 hours before testing.
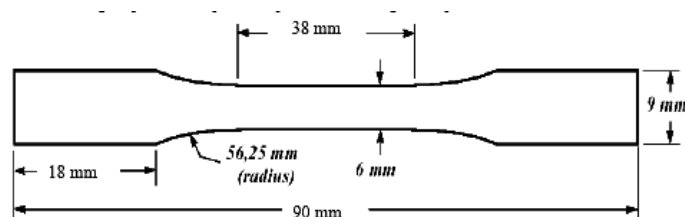

Fig.9 Probe geometry adopted about the tensile and fatigue tests

Tensile tests have been carried out at room temperature and at 600°C, fatigue tests only at room temperature, under stress-control with a max stress of 300, 500, 600 and 800 MPa (R = 0.1) with frequency of 10 Hz. Every fatigue tests have been repeated three times. Fracture surfaces have been observed by electron scanning microscopy (SEM), too.

Internal friction and dynamic modulus measurements have been carried out on bar-shaped samples using the method of frequency modulation. The VRA 1604 apparatus employed in the experiments has been described in detail in [21]. The resonance frequencies were in the range 600-1800 Hz. The samples have been heated from room temperature to 1173 K with a heating rate of 1.7 x 10^{-2} Ks^{-1}. Strain amplitude was kept lower than 1 x 10^{-5}.

Bars were mounted in free-clamped mode and put in resonance by a sinusoidal electrical excitation applied at the free end (Fig.10).
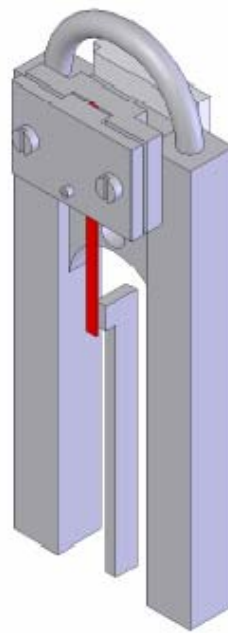

Fig.10 Internal friction experimentation: clamp system for the sample (in red)

The resonant frequency *f* has been recorded step by step while samples were heated from room temperature to 900°C with a heating rate of 1.7 x 10^{-2} °C s^{-1}.